Molecular Pharmacology Fast Forward. Published on June 26, 2012 as doi:10.1124/mol.112.079004
This article has not been copyedited and formatted. The final version may differ from this version.

Functional loss of the reduced folate carrier enhances the antitumor activities of novel antifolates with selective uptake by the proton-coupled folate transporter

Sita Kugel Desmoulin, Lei Wang, Lisa Polin, Kathryn White, Juiwanna Kushner, Mark Stout, Zhanjun Hou, Christina Cherian, Aleem Gangjee, and Larry H. Matherly

Graduate Program in Cancer Biology, Wayne State University School of Medicine, Detroit, MI 48201 (SKD, LHM)
Department of Oncology, Wayne State University School of Medicine, Detroit, MI 48201 (SKD, LP, KW, JK, ZH, CC, LHM)
Molecular Therapeutics Program, Barbara Ann Karmanos Cancer Institute, Detroit, MI 48201 (LP, ZH, CC, LHM)
Department of Pharmacology, Wayne State University School of Medicine, Detroit, MI 48201 (LHM)
Department of Pediatrics, Children's Hospital of Michigan, Detroit, MI 48201(MS)
Division of Medicinal Chemistry, Graduate School of Pharmaceutical Science, Duquesne University, Pittsburgh, PA 15282 (LW, AG)

Molecular Pharmacology Fast Forward. Published on June 26, 2012 as DOI: 10.1124/mol.112.079004
This article has not been copyedited and formatted. The final version may differ from this version.

Running title: The impact of RFC on PCFT targeted therapeutics

Address correspondence to:
Larry H. Matherly, Ph.D.
Barbara Ann Karmanos Cancer Institute
110 E. Warren Ave
Detroit, MI 48201
Tel.: 313-578-4280
Fax: 313-578-4287
Email: matherly@karmanos.org

Text pages: 22
Tables: 1
Figures: 5
References: 54
Words Abstract: 249
Introduction: 569
Discussion: 913

Non-standard abbreviations:
AICARFTase, 5-amino-4-imidazolecarboxamide ribonucleotide formyltransferase
C1, compound **1**
C2, compound **2**
dFBS, dialyzed fetal bovine serum
DPBS, Dulbecco's phosphate-buffered saline
FPGS, folylpolyglutamate synthetase
FR, folate receptor
GAPDH, glyceraldehyde-3-phosphate dehydrogenase
GAR, glycinamide ribonucleotide
GARFTase, glycinamide ribonucleotide formyltransferase
HA, hemagglutinin
HEPES, 4-(2-hydroxyethyl)-1-piperazineethanesulfonic acid
HPLC, high performance liquid chromatography
hPCFT, human proton-coupled folate transporter
hRFC, human reduced folate carrier
IC_{50}, fifty percent inhibitory concentration
5-CHO-THF, 5-formyl-tetrahydrofolate
LMX, lometrexol
MES, 4-morphilinopropane sulfonic acid
MTX, methotrexate
PCFT, proton-coupled folate transporter
PG, polyglutamate
PIPES, piperazine-N,N′-bis(2-ethanesulfonic acid)
PMX, pemetrexed
PVDF, polyvinylidene difluoride
RFC, reduced folate carrier
RTX, raltitrexed
RT-PCR, reverse transcription-PCR

Molecular Pharmacology Fast Forward. Published on June 26, 2012 as DOI: 10.1124/mol.112.079004
This article has not been copyedited and formatted. The final version may differ from this version.

SCID, severe combined immunodeficient
SEM, standard error of the mean
THF, tetrahydrofolate
WT, wild-type

Molecular Pharmacology Fast Forward. Published on June 26, 2012 as DOI: 10.1124/mol.112.079004
This article has not been copyedited and formatted. The final version may differ from this version.

ABSTRACT

Uptake of 6-substituted pyrrolo[2,3-*d*]pyrimidine thienoyl antifolates with 4 or 3 bridge carbons [compound **1** (**C1)** and compound **2** (**C2**), respectively] into solid tumors by the proton-coupled folate transporter (PCFT) represents a novel therapeutic strategy which harnesses the acidic tumor microenvironment. Although these compounds are not substrates for the reduced folate carrier (RFC), the major facilitative folate transporter, RFC expression may alter drug efficacies by impacting cellular tetrahydrofolate (THF) cofactor pools that can compete for polyglutamylation and/or binding to intracellular enzyme targets. Human tumor cells including wild-type (WT) and R5 (RFC-null) HeLa cells express high levels of PCFT protein. **C1** and **C2** inhibited proliferation of R5 cells 3 to 4 times more potently than WT cells or R5 cells transfected with RFC. Transport of **C1** and **C2** was virtually identical between WT and R5 cells, establishing that differences in drug sensitivities between sublines were independent of PCFT transport. Steady-state intracellular [^{3}H]THF cofactors derived from [^{3}H]5-formyl-THF were depleted in R5 cells compared to WT cells, an effect exacerbated by **C1** and **C2**. While **C1** and **C2** polyglutamates accumulated to similar levels in WT and R5 cells, there were differences in polyglutamyl distributions in favor of the longest chain-length forms. In severe combined immunodeficient mice, anti-tumor efficacies of **C1** and **C2** were greater toward subcutaneous R5 tumors compared to WT tumors, confirming the collateral drug sensitivities observed *in vitro*. Thus, solid tumor-targeted antifolates with PCFT-selective cellular uptake should have enhanced activities toward tumors lacking RFC function, reflecting contraction of THF cofactor pools.

Molecular Pharmacology Fast Forward. Published on June 26, 2012 as DOI: 10.1124/mol.112.079004
This article has not been copyedited and formatted. The final version may differ from this version.

INTRODUCTION

Classical antifolates such as methotrexate (MTX) and pemetrexed (PMX), like folate cofactors, have minimal lipid solubility and therefore require specific transport mechanisms to enter mammalian cells. There are three primary folate transporters, including the reduced folate carrier (RFC), the proton-coupled folate transporter (PCFT) and folate receptor (FR) α (Assaraf, 2007; Goldman et al., 2010). RFC is the predominant transport route for the major circulating folate, 5-methyl tetrahydrofolate (THF), and (6S) 5-formyl THF (5-CHO-THF) in mammalian cells and tissues (Matherly et al., 2007). RFC also mediates cellular uptake of MTX and is essential to MTX antitumor activity (Matherly et al., 2007). Impaired RFC function is a major mechanism of MTX resistance in cultured tumor cells selected *in vitro* (Matherly et al., 2007; Zhao and Goldman, 2003) and in murine leukemia cells *in vivo* (Sirotnak et al., 1981). Loss of RFC function in clinical specimens has also been reported (Gorlick et al., 1997; Guo et al., 1999; Yang et al., 2003). RFC transport of cytotoxic antifolates can also be undesirable since RFC is ubiquitously expressed and exhibits a high level of activity at the neutral pHs characterizing most normal tissues (Matherly et al., 2007). Thus, transport of antifolates by RFC could easily preclude tumor selectivity and cause toxicity to normal tissues.

The novel 6-substituted pyrrolo[2,3-*d*]pyrimidine thienoyl antifolates with 4 [compound **1** (**C1**)] or 3 [compound **2** (**C2**)] carbon bridge lengths (Figure 2A) represent a new class of antitumor agents that exhibit a lack of significant membrane transport by RFC (Kugel Desmoulin et al., 2011; Wang et al., 2010; Wang et al., 2011). Cellular uptake of **C1** and **C2** by PCFT and FRα is efficient and offers a promising new strategy for solid tumor targeting (Anderson and Thwaites, 2010; Kugel Desmoulin et al., 2011). Since PCFT

Molecular Pharmacology Fast Forward. Published on June 26, 2012 as DOI: 10.1124/mol.112.079004
This article has not been copyedited and formatted. The final version may differ from this version.

functions optimally at acidic pHs (Qiu et al., 2006; Umapathy et al., 2007; Zhao et al., 2008), transport of **C1** and **C2** by PCFT may lead to further enhancement of tumor selectivity owing to the acidic microenvironments of many solid tumors (Anderson and Thwaites, 2010; Gillies et al., 2002; Helmlinger et al., 1997; Webb et al., 2011). Our previous results established that **C1** and **C2** are potent inhibitors of tumor cell proliferation both *in vitro* and *in vivo* (Kugel Desmoulin et al., 2011; Wang et al., 2010; Wang et al., 2011).

For agents such as PMX that are excellent substrates for both RFC and PCFT, loss of RFC has limited impact on overall activity, since PMX uptake is maintained by PCFT (Zhao et al., 2004c; Zhao et al., 2008). Paradoxically, RFC loss has been shown to enhance antitumor activity (i.e., collateral sensitivity) of PMX via decreased intracellular THF cofactor pools (Chattopadhyay et al., 2007; Chattopadhyay et al., 2006; Zhao et al., 2004c). This response to RFC loss can be further impacted by the type and amount of extracellular folate (Chattopadhyay et al., 2006; Zhao et al., 2004b; Zhao et al., 2004c).

An analogous effect may exist for PCFT-selective substrates such as **C1** and **C2**, although this has never been systematically tested. In this report, we examine the complex interplay between RFC and extracellular reduced folates. Specifically, we investigate the mechanistic ramifications of loss of RFC function toward *in vitro* and *in vivo* antitumor efficacies of these novel PCFT-targeted antifolates. Our results strongly imply that levels of folate transport by RFC in tumors are critical determinants of drug efficacy for this novel class of PCFT-selective antitumor agents.

Molecular Pharmacology Fast Forward. Published on June 26, 2012 as DOI: 10.1124/mol.112.079004
This article has not been copyedited and formatted. The final version may differ from this version.

MATERIALS AND METHODS

Materials. [3',5',7-^{3}H]MTX (20 Ci/mmol), [^{3}H]PMX (2.5 Ci/mmol), [3',5',7,9-^{3}H(N)](6S)5-formyl tetrahydrofolate (5-CHO-THF) (16.6 Ci/mmol), and custom-radiolabeled [^{3}H]**C1** (1.3 Ci/mmol) and [^{3}H]**C2** (16 Ci/mmol) were purchased from Moravek Biochemicals. Sources of the non-radioactive folate and antifolate drugs are summarized in Table 1S (Supplement).

Cell lines. The sources and cell culture conditions for assorted human solid tumor cell lines are summarized in Table 2S (Supplement). HeLa cells were obtained commercially. RFC-null R5 HeLa cells were previously described (Zhao et al., 2004b). R1-11-mock and R1-11-PCFT4 HeLa cells were derived from human RFC (hRFC)- and hPCFT-null R1-11 cells by stable transfection with pZeoSV2(+) vector (Invitrogen) only, or with hemagglutinin (HA)-tagged hPCFT in pZeoSV2(+), respectively. Characteristics and culture conditions of the engineered HeLa sublines were described (Zhao et al., 2008) and are also in Table 2S (Supplement).

Preparation of hRFC^{HA}/pZeoSV2 and generation of stable hRFC R5 transfectants. Full-length hRFC was subcloned using BamHI and Xho1 into pZeoSV2(+) in-frame with a C-terminal HA sequence to generate hRFC^{HA}/pZeoSV2. The plasmid was transformed into XL10-Gold ultracompetent cells (Agilent) and selected using low salt LB agar plates containing 25 μg/ml Zeocin. Plasmids were isolated and the wild-type (WT) hRFC insert confirmed by DNA sequencing by Genewiz Corp. (South Plainfield, NJ).

Molecular Pharmacology Fast Forward. Published on June 26, 2012 as DOI: 10.1124/mol.112.079004
This article has not been copyedited and formatted. The final version may differ from this version.

R5 cells were transfected with pZeoSV2 vector control or $hRFC^{HA}$/pZeoSV2 with Lipofectamine 2000 and opti-MEM (Invitrogen). After 24 h, the cells were cultured with zeocin (0.1 mg/ml). Stable clones were selected by plating for individual colonies in the presence of 0.1 mg/ml zeocin. Colonies were isolated, expanded and screened for expression of $hRFC^{HA}$ by real-time reverse transcription-PCR (RT-PCR), Western blotting and transport assays at pH 7.2 (below). A representative clone (R5-RFC2) was selected for further study. R5 cells transfected with empty pZeoSV2 (R5-mock) were also prepared.

Gel electrophoresis and western blotting. To characterize hPCFT and hRFC protein levels in assorted human solid tumor cell lines and the R5-RFC transfectants, plasma membranes were prepared by differential centrifugation and sucrose-density centrifugation (Matherly et al., 1991). Proteins were quantified with Folin-phenol reagent (Lowry et al., 1951).

Membrane proteins were electrophoresed on 7.5% polyacrylamide gels with SDS (Laemmli, 1970) and electroblotted onto polyvinylidene difluoride (PVDF) membranes (Pierce) (Matsudaira, 1987). For detecting total immunoreactive hPCFT and hRFC proteins on PVDF membranes, hPCFT or hRFC-specific polyclonal antibodies raised in rabbits to carboxyl-termini hPCFT or hRFC (Hou et al., 2011; Wong et al., 1998) peptides, and an IRDye800CW-conjugated goat anti-rabbit IgG (Rockland) secondary antibody were used. For detecting HA-tagged proteins (i.e., $R5\text{-}RFC^{HA}$), HA-specific mouse monoclonal antibody (Covance) and an IRDye800CW-conjugated goat anti-mouse IgG (Rockland) secondary antibody were used. Membranes were scanned with the

Molecular Pharmacology Fast Forward. Published on June 26, 2012 as DOI: 10.1124/mol.112.079004
This article has not been copyedited and formatted. The final version may differ from this version.

Odyssey® infrared imaging system. hPCFT and hRFC levels were normalized to levels of Na^+/K^+ ATPase (Novus Biologicals).

Transport assays. To assay hPCFT transport in assorted solid tumor cell lines, uptake of 0.5 μM [^{3}H]MTX was measured in cell monolayers in 60 mm dishes over 5 min at 37°C. The transport buffer was 4-morphilinopropane sulfonate (MES)-buffered saline (20 mM MES, 140 mM NaCl, 5 mM KCl, 2 mM $MgCl_2$, and 5 mM glucose) at pH 5.5 (Zhao et al., 2004b). Some transport experiments were performed with 20 nM folic acid to exclude cellular uptake by FRs.

The pH-dependent uptake of [^{3}H]**C1,** [^{3}H]**C2,** [^{3}H]PMX or [^{3}H]MTX (0.5 μM) in the HeLa sublines was assayed at 37^{o}C in cell monolayers over 2 min at 37°C in 2 ml "anion-free" 4-(2-hydroxyethyl)-1-piperazineethanesulfonic acid (HEPES)-sucrose-Mg^{+2} buffer (20 mM HEPES, 235 mM sucrose, pH adjusted to 7.14 with MgO) (AFB) (Wong et al., 1997), HEPES-buffered saline (20 mM HEPES, 140 mM NaCl, 5 mM KCl, 2 mM $MgCl_2$, and 5 mM glucose, pH 6.8), or in MES-buffered saline (pH 5.5). Transport fluxes were stopped by aspirating the buffer and quenching with excess (> 5 ml) ice-cold Dulbecco's phosphate-buffered saline (DPBS), followed by 3 washes with DPBS. Cellular proteins were solubilized with 0.5 N NaOH and quantified with Folin-phenol reagent (Lowry et al., 1951). Drug uptake was expressed as pmol/mg protein, calculated from measurements of radioactivity with a scintillation counter and the protein contents of the cell homogenates.

Molecular Pharmacology Fast Forward. Published on June 26, 2012 as DOI: 10.1124/mol.112.079004
This article has not been copyedited and formatted. The final version may differ from this version.

To measure PCFT transport kinetics (K_t and V_{max}) for [^{3}H]**C2** in engineered R1-11-PCFT4 HeLa cells, cells were grown in spinner flasks, collected by centrifugation, washed with DPBS, and suspended (at 1.5 x 10^7 cells) in 2 ml MES-buffered saline at pH 5.5 containing [^{3}H]**C2** substrate concentrations ranging from 0.04 to 5 μM. K_t and V_{max} values were determined from Lineweaver-Burke plots. Kinetic constants for **C2** were compared to those previously published in R1-11-PCFT4 cells for **C1** and PMX (Kugel Desmoulin et al., 2011).

Real-time RT-PCR analysis of RFC, FR*α*, and PCFT transcripts. RNAs were prepared from WT, R5 and R5-RFC2 HeLa cells using TRIZOL reagent (Invitrogen). cDNAs were synthesized using random hexamers, RNase inhibitor, and MuLV reverse transcriptase and purified with the QIAquick PCR Purification Kit (Qiagen). Quantitative real-time RT-PCR was performed on a Roche LightCycler 1.2 (Roche) with gene-specific primers and FastStart DNA Master SYBR Green I reaction mix (Roche) (Ge et al., 2007). Primers are in Table 3S (Supplement). Transcript levels for hRFC were normalized to those for glyceraldehyde-3-phosphate dehydrogenase (GAPDH). External standard curves were constructed for each gene of interest using serial dilutions of linearized templates, prepared by amplification from suitable cDNA templates, subcloning into a TA-cloning vector (PCR-Topo; Invitrogen), and restriction digestions.

Cell proliferation assays. For proliferation assays, WT and the R5 HeLa sublines were cultured in folate-free RPMI 1640 (pH 7.2), supplemented with 10% dialyzed fetal bovine serum (dFBS), 2 mM L-glutamine and 100 units/ml penicillin/100 μg/ml streptomycin (hereafter referred to as “complete folate-free RPMI 1640 medium”),

Molecular Pharmacology Fast Forward. Published on June 26, 2012 as DOI: 10.1124/mol.112.079004
This article has not been copyedited and formatted. The final version may differ from this version.

containing 25 nM 5-CHO-THF, for at least 2 weeks prior to experiment. For drug inhibition assays, the cells were plated in 96 well culture dishes (2500 cells/well; 200 μl/well) in the above medium with a range of drug concentrations; cells were incubated for up to 96 h at 37^{o}C in a CO_2 incubator. Cell numbers were assayed with Cell Titer Blue™ cell viability assays (Promega) with a fluorescent plate reader for determining IC_{50}s (drug concentrations that result in 50% loss of cell growth). To test the impact of extracellular folates on the collateral sensitivities of **C1** and **C2** in the HeLa sublines, some growth inhibition experiments included increasing concentrations (25, 100, 1000 nM) of 5-CHO-THF.

Accumulation of [^{3}H]5-CHO-THF. WT and R5 HeLa sublines were cultured in complete folate-free RPMI 1640 supplemented with 0.06 mM adenosine and 0.01 mM thymidine for five days prior to the experiment. Adenosine and thymidine were added in to circumvent folate requirements and to maintain cell viability in the absence of exogenous folates. Cells were treated with 0, 25, 100 and 1000 nM [^{3}H]5-CHO-THF (since [^{3}H] (6S)5-CHO-THF was diluted with non-radioactive (6R,S)5-CHO-THF for these experiments, the actual concentration of (6S) stereoisomer was 12.5, 50, 500 nM, respectively) for four days, followed by 3 washes with ice-cold DPBS. A control without added [^{3}H]5-CHO-THF (including 0.06 mM adenosine and 0.01 mM thymidine) was incubated in parallel. Cellular proteins were solubilized with 0.5 N NaOH and quantified using Folin-phenol reagent (Lowry et al., 1951). Total cellular [^{3}H]5-CHO-THF accumulations were expressed as pmol/mg protein, calculated from direct measurements of radioactivity and protein contents of cell homogenates. Since [^{3}H](6S)5-CHO-THF was diluted with unlabeled (6R,S)5-CHO-THF (see above), for purposes of calculating

Molecular Pharmacology Fast Forward. Published on June 26, 2012 as DOI: 10.1124/mol.112.079004
This article has not been copyedited and formatted. The final version may differ from this version.

intracellular folate metabolites only the unlabeled (6S) isomer was considered. To measure the impact of the PCFT-targeted therapeutics **C1** and **C2** on [^{3}H]5-CHO-THF accumulations, some experiments analyzed the uptake of 25 nM [^{3}H]5-CHO-THF in the presence of increasing concentrations (0-1000 nM) of compounds **C1** and **C2** in complete folate-free RPMI 1640 supplemented with 0.06 mM adenosine.

Measurement of C1 and C2 polyglutamylation. WT and R5 HeLa cells were depleted of folates by growth for 2 weeks in complete folate-free RPMI plus 25 nM 5-CHO-THF. Cells were plated in media without nucleosides, supplemented with 25 nM 5-CHO-THF, and allowed to adhere overnight. Cells were washed with DPBS and incubated in the same media, with 25 mM piperazine-N,N′-bis(2-ethanesulfonic acid (PIPES)/25 mM HEPES (pH 6.8), 0.06 mM adenosine and 1 μM [^{3}H]**C1** or [^{3}H]**C2.** After 16 h, cells were washed three times with ice-cold DPBS and scraped into 5 ml of DPBS, pelleted (1500 rpm) and flash-frozen. Polyglutamyl and unmetabolized drug forms were extracted and levels quantified by HPLC (Kugel Desmoulin et al., 2011). Cellular proteins were quantified with Folin-phenol reagent (Lowry et al., 1951). Polyglutamyl and parent drug forms were normalized to cellular proteins and expressed as pmol/mg cell protein.

***In vivo* efficacy study of C1 and C2 in WT and R5 HeLa xenografts**. Cultured WT and R5 HeLa cells were implanted subcutaneously (~ 10^7 cells/flank) to establish a solid tumor xenograft model (passage 0) in female ICR SCID mice (National Institutes of Health DCT/DTP Animal Production Program, Frederick, MD). The mice were supplied food and water *ad libitum.* Study mice were maintained on a folate-deficient diet (Harlan-Teklad; Product ID: TD.00434) starting 18 days before tumor implant to ensure serum

Molecular Pharmacology Fast Forward. Published on June 26, 2012 as DOI: 10.1124/mol.112.079004
This article has not been copyedited and formatted. The final version may differ from this version.

folate levels would approximate those of humans prior to the start of therapy (Kugel Desmoulin et al., 2011; Wang et al., 2010; Wang et al., 2011). This design is analogous to those previously published by others (Alati et al., 1996; Gibbs et al., 2005).

For the efficacy trial, the experimental animals were pooled, divided into groups (4 mice/group), and implanted bilaterally subcutaneously with 30-60 mg tumor fragments (from passage 3) using a 12-gauge trocar. Chemotherapy began on day 3 post tumor implantation, when the number of cells was between 10^7-10^8 cells (below the limit of palpation). An organic solvent (ethanol, 5% v/v), carrier (Tween-80, 1% v/v) and sodium bicarbonate (0.5% v/v) were used to effect solubilization of **C1** and **C2.** Injection volumes were 0.2 ml IV. Tumors were measured with a caliper two to three times weekly. Mice were sacrificed when cumulative tumor burdens reached 1500 mg. Methods of protocol design, drug treatments, toxicity evaluation, and data analysis were described (Corbett et al., 1998; Corbett et al., 1997; Polin et al., 2011; Polin et al., 1997). Experimental parameters as qualitative and quantitative end points to assess antitumor activities include T/C in percent (see legend of Table 1 for further details) and T-C (tumor growth delay) [where T is the median time in days required for the treatment group tumors to reach a predetermined size (e.g., 1000 mg) and C is the median time in days for the control group tumors to reach the same size; tumor-free survivors are excluded from these calculations], and tumor cell kill [$\log_{10}$ cell kill total (gross) = (T - C)/(3.32)(Td), where (T – C) is the tumor growth delay, as described above, and Td is the tumor volume doubling time in days, estimated from the best fit straight line from a log-linear growth plot of control group tumors in exponential growth (100-800 mg range)]. The day of tumor implant was day 0. For comparison of antitumor activities with

Molecular Pharmacology Fast Forward. Published on June 26, 2012 as DOI: 10.1124/mol.112.079004
This article has not been copyedited and formatted. The final version may differ from this version.

standard agents or between tumors, $\log_{10}$ kill values were converted to an arbitrary activity rating (Corbett et al., 1997). With the exception of the xenograft model, these methods are essentially identical to those described previously (Kugel Desmoulin et al., 2011; Wang et al., 2010; Wang et al., 2011).

Statistical analysis. Statistical analyses were performed with GraphPad Instat 2.0.

RESULTS

Expression and function of hRFC and hPCFT in human solid tumor cell lines. We previously measured substantial levels of hPCFT transcripts by real-time RT-PCR in 52 of 53 human solid tumor cell lines of different origins (e.g., breast, prostate, ovarian, etc.) (Kugel Desmoulin et al., 2011). As an extension of this work, we measured levels of hPCFT proteins for ten of the tumor cell lines (HepG2, Hep3B, H596, CRL5810, H2595, HCT15, Caco-2, DU145, MDA-MB 321, and SK-MEL5) (Table 1S, Supplement). We also analyzed four HeLa sublines, including WT and hRFC-null R5 cells, both of which express hPCFT, and two HeLa sublines derived from hRFC- and hPCFT-null R1-11 cells including R1-11-mock (hereafter, R1-11) and R1-11-PCFT4 (R1-11 cells stably transfected with hPCFT) cells. For each cell line, plasma membrane proteins were separated by SDS-PAGE and immunoblotted with hPCFT-specific antibodies. Levels of heterogeneously glycosylated hPCFT proteins detected by western blotting (Figure 1A) paralleled those of hPCFT transcripts (Kugel Desmoulin et al., 2011). hPCFT proteins were detected in all tumor cell lines except for the parental R1-11 cells.

Molecular Pharmacology Fast Forward. Published on June 26, 2012 as DOI: 10.1124/mol.112.079004
This article has not been copyedited and formatted. The final version may differ from this version.

Functional validation of hPCFT expression in the solid tumor cell lines was established by transport assays with [^{3}H]MTX (0.5 μM, 5 min) at pH 5.5 (Figure 1B). Substantial [^{3}H]MTX uptake at pH 5.5 was detected in cell lines expressing hPCFT protein with the highest levels in Hep3B and Caco-2, accompanying elevated PCFT protein levels.

hPCFT transport of [^{3}H]C2 in R1-11-PCFT4 cells. We previously found that the novel 6-substituted pyrrolo[2,3-*d*]pyrimidine thienoyl antifolates **C1** and **C2** (Figure 2A) were potent (nM) inhibitors of proliferation in cells engineered to express hPCFT in the absence of hRFC or FRs (Kugel Desmoulin et al., 2011; Wang et al., 2010; Wang et al., 2011), suggesting that **C1** and **C2** are substrates for hPCFT-mediated cellular uptake. In engineered cell lines, **C1** and **C2** appeared to be poorly transported by hRFC (Kugel Desmoulin et al., 2011; Wang et al., 2010; Wang et al., 2011). Both analogs induced current at -90 mV and pH 5.5 in *Xenopus* oocytes microinjected with hPCFT cRNAs, and both were competitive inhibitors of [^{3}H]MTX transport in hPCFT transfectants from pH 5.5 to pH 6.8 (Kugel Desmoulin et al., 2011; Wang et al., 2011). Transport of [^{3}H]**C1** by hPCFT was directly demonstrated in R1-11-PCFT4 cells (Kugel Desmoulin et al., 2011).

To confirm hPCFT transport of **C2**, R1-11-PCFT4 cells were incubated with [^{3}H]**C2** (0.5 μM, 5 min, 37^o C) at pH 5.5 and 6.8 in the presence and absence of unlabeled **C1** (10 μM) as a competitive inhibitor. Transport was detected at a ~4-fold higher level at pH 5.5 than at pH 6.8, and at both pHs uptake was substantially inhibited in the presence of *unlabeled* **C1** (Figure 2B). These results establish that **C2**, like its 4-carbon chain homolog, **C1**, is a *bona fide* substrate for membrane transport by hPCFT. Transport kinetic parameters for **C2** with R1-11-PCFT4 cells at pH 5.5 are summarized in Table 4S

Molecular Pharmacology Fast Forward. Published on June 26, 2012 as DOI: 10.1124/mol.112.079004
This article has not been copyedited and formatted. The final version may differ from this version.

(Supplement). K_t and V_{max} values for **C2** were similar to those previously reported for **C1** and PMX (Kugel Desmoulin et al., 2011).

Transport and membrane expression of hPCFT and hRFC in WT and R5 HeLa sublines. While **C1** and **C2** are not RFC transport substrates (Kugel Desmoulin et al., 2011; Wang et al., 2010; Wang et al., 2011), RFC levels could nonetheless markedly impact the anti-proliferative effects of these agents, via expansion or contraction of intracellular THF cofactor pools. Thus, RFC levels or ratios of PCFT to RFC transport might effectively predict antitumor potencies of these prototypical PCFT-targeted antifolates. This could be further impacted by varying concentrations of extracellular THF cofactors.

To explore this concept, we used WT and R5 HeLa cells which express comparable levels of hPCFT with or without hRFC (Figure 1, Figure 3A, and Figure 1SA). R5 cells are resistant to MTX (Figure 5A) because of a genomic deletion that results in loss of hRFC (Zhao et al., 2004a). MTX resistance is completely reversible upon transfection with WT hRFC (R5-RFC2 cells), which restores hRFC transport (Figure 1SB), confirming that loss of hRFC transport is causal to the resistant phenotype.

While [^{3}H]MTX (0.5 μM) transport by hPCFT at pH 5.5 was nearly identical for WT and R5 HeLa cells (Figure 3B), MTX uptake in R5 cells in AFB at pH 7.2 was decreased ~3-fold compared to WT cells (Figure 3C), consistent with the loss of hRFC. Ratios of MTX transport at pH 5.5 (PCFT) to pH 7.2 (RFC) for R5 and WT cells were ~11 and ~3, respectively (Figure 3D). Transport was also measured for [^{3}H]**C1** and [^{3}H]**C2** (both at

Molecular Pharmacology Fast Forward. Published on June 26, 2012 as DOI: 10.1124/mol.112.079004
This article has not been copyedited and formatted. The final version may differ from this version.

0.5 μM; 2 min, 37°C) and for [^{3}H]PMX at pH 5.5 and pH 7.2. Results were compared to those for [^{3}H]MTX (Figures 3B and 3C). For all compounds and both cell lines, transport by hPCFT over hRFC predominated, as uptake showed the characteristic pH dependence for PCFT with the highest levels at pH 5.5. While there were slight differences in initial rates of uptake of the various analogs at pH 5.5, these were not statistically significant. Further, there were no obvious differences in membrane transport of the individual analogs between WT and R5 HeLa cell lines.

Impact of hRFC and extracellular folate on antitumor activities of C1 and C2. (6S) 5-CHO-THF is poorly transported by PCFT at neutral pH and is less effective in supporting proliferation of PCFT-expressing cells (without RFC) than RFC-expressing cells (without PCFT) (Zhao et al., 2008). Thus, loss of hRFC in R5 cells would be predicted to contract intracellular pools of reduced folates derived from 5-CHO-THF, compared to those in WT HeLa cells (Chattopadhyay et al., 2006; Zhao et al., 2004b). This effect may be exacerbated in the presence of high affinity hPCFT-selective substrates which could further restrict the modest levels of THF cofactor uptake via PCFT through direct competition.

To examine these possibilities, folate-depleted WT, R5 and R5-RFC2 cells were cultured in 25, 100, or 1000 nM [^{3}H]5-CHO-THF [corresponding to 12.5, 50, or 500 nM of the active (6S) stereoisomer] for 96 h in order to determine cellular accumulations of [^{3}H]THF metabolites. During sustained culture, the media pH decreased to ~6.8 (Kugel Desmoulin et al., 2010) and was accompanied by dose-dependent accumulations of [^{3}H]5-CHO-THF (Figure 4A). At 25 nM [^{3}H]5-CHO-THF, R5 cells experienced a 31.6%

Molecular Pharmacology Fast Forward. Published on June 26, 2012 as DOI: 10.1124/mol.112.079004
This article has not been copyedited and formatted. The final version may differ from this version.

decreased net accumulation of tritiated folates compared to WT cells ($p<0.05$), and a 49.6% decrease compared to R5-RFC2 cells ($p<0.05$). While this difference between WT and R5 cells decreased at 100 nM and 1000 nM [^{3}H]5-CHO-THF, statistically significant differences in [^{3}H]5-CHO-THF accumulations were preserved at these concentrations between R5 and R5-RFC2 cells (Figure 4A).

We measured proliferation of WT and R5 HeLa cells grown in 25 nM 5-CHO-THF in the presence of range of concentrations (0 to 1000 nM) of the PCFT-selective antifolates **C1** and **C2**, for comparison with MTX, lometrexol (LMX), raltitrexed (RTX), and PMX, classical antifolates which are transported by both RFC and PCFT (Goldman et al., 2010; Kugel Desmoulin et al., 2011; Kugel Desmoulin et al., 2010), and with PT523, which is transported by RFC but not PCFT (Kugel Desmoulin et al., 2011; Kugel Desmoulin et al., 2010; Zhao and Goldman, 2007). Similar to published results (Zhao et al., 2004c), R5 (and R5 mock-transfected) cells were substantially resistant to PT523 compared to WT (> 213-fold) and R5-RFC2 (> 303-fold) cells (Figure 5A and Table 5S). Further, R5 cells were resistant (5- to 14-fold) to MTX, LMX, and RTX compared to WT HeLa cells. For PMX, IC_{50}s for WT and R5 cells were modestly different (IC_{50}s of 48.3 and 66.1 nM, respectively). Notably, hRFC-deficient R5 cells were substantially *more sensitive* to the PCFT-specific antifolates **C1** and **C2** than were WT cells (3.6- and 3.2-fold, respectively) and the R5-RFC2 transfected cells (3.6- and 8.3-fold, respectively). While differences in growth inhibitions between R5 and WT cells for **C1** and **C2** were preserved when the extracellular 5-CHO-THF was increased to 100 nM (4.3- and 15-fold, respectively), the effects of both drugs were effectively abolished when the 5-CHO-THF concentration was increased to 1000 nM (Figure 5B and C).

Molecular Pharmacology Fast Forward. Published on June 26, 2012 as DOI: 10.1124/mol.112.079004
This article has not been copyedited and formatted. The final version may differ from this version.

Since **C1** and **C2** are high affinity substrates for PCFT, we hypothesized that these drugs compete with [^{3}H]5-CHO-THF for PCFT uptake, leading to a more severe contraction of the cellular folate pool in R5 cells compared to WT cells than in their absence. Indeed, both **C1** and **C2** affected a striking dose-dependent decrease in net accumulations of [^{3}H]5-CHO-THF which were greater in hRFC-null R5 cells than in WT HeLa cells. At 1000 nM **C1**, levels of [^{3}H]5-CHO-THF accumulation in R5 and WT HeLa cells were 52.9% and 72.9%, respectively, of levels without drug; for **C2**, the corresponding values were 52.7% and 71.1%, respectively (Figure 4B and C).

Collectively, these results establish that loss of hRFC contributes to a contraction of cellular folate pools which is exacerbated in the presence of the PCFT-selective analogs **C1** and **C2**. Importantly, decreased intracellular folates were accompanied by markedly increased antiproliferative effects of **C1** and **C2**.

Polyglutamylation of C1 and C2 in WT and R5 HeLa cells. Analogous to physiologic folates and other classic antifolate drugs such as MTX (Assaraf, 2007; Goldman and Matherly, 1985; Shane, 1989), **C1** is metabolized to polyglutamates (PGs) (Kugel Desmoulin et al., 2011). Polyglutamylation of **C2** has not been previously assessed. As polyglutamylation of antifolate drugs by folylpolyglutamate synthetase (FPGS) can be regulated by elevated extra- and intracellular folates (Tse and Moran, 1998; Zhao et al., 2001), it seemed possible that the impact of hRFC and cellular THF cofactors on the anti-proliferative effects of **C1** and **C2** may be partly explained in this manner.

Molecular Pharmacology Fast Forward. Published on June 26, 2012 as DOI: 10.1124/mol.112.079004
This article has not been copyedited and formatted. The final version may differ from this version.

To assess this possibility, WT and R5 HeLa cells were incubated with 1 μM [^{3}H]**C1** or [^{3}H]**C2** for 16 h at pH 6.8 in the presence of 25 nM 5-CHO-THF and 0.06 mM adenosine. Total cellular radiolabeled drug levels were quantified and tritiated parent drug and PGs were extracted and analyzed. At least four polyglutamyl metabolites (PG_{2-5}) of [^{3}H]**C1** and five metabolites for [^{3}H]**C2** (PG_{2-6}) were resolved by HPLC. Migrations were compared to those for non-polyglutamyl **C1** or **C2**, and to MTX and MTX PG standards. Further, samples were treated in parallel with conjugase (Kugel Desmoulin et al., 2011), which reverted the majority of the polyglutamyl metabolites to the parental drugs (not shown). Results are summarized in Figure 2S (Supplement). HPLC chromatograms for the radiolabeled drug forms in HeLa and R5 cells are shown in Figure 3S (Supplement). For R5 and WT cells, there was a 7-8-fold greater accumulation of total and polyglutamyl [^{3}H]**C2** than for [^{3}H]**C1**. WT and R5 cells accumulated similar levels of total **C1** and **C2** drug forms, although there were slight differences in relative accumulations of individual PGs between the cell lines. This difference was most obvious for the longest chain-length PGs (PG_5 and PG_6) and was somewhat greater for **C1** than for **C2**.

These results establish that: (i) both **C1** and **C2** are excellent substrates for polyglutamylation under conditions (pH 6.8) that favor their membrane transport by PCFT; (ii) net drug accumulation and polyglutamylation of **C2** far exceeds that for **C1**; and (iii) the presence or absence of functional RFC manifests at most a modest effect on net **C1** and **C2** polyglutamate synthesis.

Molecular Pharmacology Fast Forward. Published on June 26, 2012 as DOI: 10.1124/mol.112.079004
This article has not been copyedited and formatted. The final version may differ from this version.

***In vivo* efficacy of C1 and C2 against WT and R5 HeLa xenografts.** To extend our *in vitro* cell proliferation studies *in vivo*, we performed *in vivo* antitumor efficacy studies with 8 week old female ICR SCID mice implanted with subcutaneous R5 or WT HeLa cells. Mice were maintained *ad libitum* on a folate-deficient diet which decreased serum folates to levels approximating those seen in humans. For the efficacy trial, control and drug treatment groups were non-selectively randomized (four mice/group); **C1** or **C2** were administered intravenously (180 and 32 mg/kg per injection, respectively) on days 3, 7, 14 and 18 post-implantation. As reported for other tumor models (Kugel Desmoulin et al., 2011; Wang et al., 2011), **C1** and **C2** showed substantial efficacies toward R5 and WT HeLa xenografts (Table 1). Both **C1** and **C2** showed greater efficacies toward R5 cells (T-C = 23 days, 3.3 gross $\log_{10}$ kill for **C1**; T-C = 17.5 days, 2.5 gross $\log_{10}$ kill for **C2**) than toward WT cells (T-C = 13 days, 1.9 gross $\log_{10}$ kill for **C1**; T-C = 13 days, 1.9 gross $\log_{10}$ kill for **C2**). Differences in C-T and $\log_{10}$ kill results between R5 and WT HeLa cells for compound **C1** were statistically significant ($p=0.014$ and $p=0.0135$, respectively). However, differences in these parameters for **C2** did not quite reach statistical significance ($p=0.146$). The treatment regimens with **C1** and **C2** were well tolerated with dose-limiting symptoms manifesting as reversible body weight loss.

The results of the *in vivo* efficacy trial provide proof-of-principle confirmation of our *in vitro* findings that the antitumor effects of both **C1** and **C2** are greater in hRFC-deficient R5 cells than in WT cells. Interestingly, the impact of loss of hRFC appears to be somewhat greater with **C1** than with **C2** *in vivo*.

Molecular Pharmacology Fast Forward. Published on June 26, 2012 as DOI: 10.1124/mol.112.079004
This article has not been copyedited and formatted. The final version may differ from this version.

DISCUSSION

In this study, we expanded upon previous reports (Goldman et al., 2010; Kugel Desmoulin et al., 2011; Kugel Desmoulin et al., 2010; Wang et al., 2010; Wang et al., 2011; Zhao and Goldman, 2007) that hPCFT may be exploitable for cancer therapy, reflecting unique patterns of hPCFT expression and appreciable transport activity at pHs approximating the tumor microenvironment. We extended our previous findings establishing broad-ranging hPCFT gene expression in a large number of human tumor cell lines (Kugel Desmoulin et al., 2011) to include measurements of hPCFT protein and transport activity. Our results document that hPCFT protein levels are abundantly expressed, accompanying substantial transport activities at pH 5.5.

We demonstrated that functional loss of hRFC in R5 cells caused a contraction of total cellular THF cofactor pools derived from 5-CHO-THF which enhanced both **C1** and **C2** antitumor activities compared to WT cells. Importantly, reduction of total cellular folate pools in R5 cells was exacerbated in the presence of **C1** and **C2**, through direct competition at hPCFT, which further restricted cellular uptake of exogenous 5-CHO-THF. Efficacies of **C1** and **C2** were also increased toward R5 tumors compared to WT tumors transplanted into SCID mice with serum folate concentrations approximating those achieved in humans, although this appeared to be somewhat greater with **C1** than with **C2** *in vivo*. We previously reported that the *in vivo* efficacy of **C2** toward IGROV1 xenogafts in SCID mice was less impacted by serum folates than for **C1** (Wang et al., 2010; Wang et al., 2011).

Molecular Pharmacology Fast Forward. Published on June 26, 2012 as DOI: 10.1124/mol.112.079004
This article has not been copyedited and formatted. The final version may differ from this version.

There is ample precedent for an impact of folate pools on antifolate drug efficacy. Indeed, this is the premise of leucovorin rescue from MTX toxicity (Matherly et al., 1987) and of low-dose folic acid protection from LMX toxicity *in vivo* (Roberts et al., 2000), whereby elevated extra- and intracellular folates compete at multiple levels to reverse drug activity. *In vitro* studies have extended these findings to both classical (PMX, LMX) and non-classical (trimetrexate) antifolates, which inhibit a range of cellular targets (Goldman et al., 2010; Tse and Moran, 1998; Zhao et al., 2001). Further, antifolate drug activities are enhanced by decreased intracellular folates resulting from an hRFC genomic deletion (Chattopadhyay et al., 2006; Zhao et al., 2004b; Zhao et al., 2004c) or hRFC mutations (Zhao et al., 2000a). Similarly, antifolate effects are reduced by increased intracellular folates resulting from impaired efflux of folic acid (Assaraf and Goldman, 1997) or enhanced folic acid influx by a mutant RFC (Tse et al., 1998; Tse and Moran, 1998).

Regardless of the underlying mechanism and intracellular drug target involved, markedly decreased total intracellular THF pools can result in collateral sensitivities to antifolates, often in the face of substantially decreased levels of drug uptake (Chattopadhyay et al., 2006; Zhao et al., 2000b; Zhao et al., 2001; Zhao et al., 2004c). This could reflect inhibitory effects on drug polyglutamylation (with consequent impact on drug retention and inhibition of folate-dependent enzyme targets) due to competitive feedback inhibition at FPGS by high levels of THF cofactor PGs (Nimec and Galivan, 1983; Shane, 1989; Tse and Moran, 1998; Zhao et al., 2001; Zhao et al., 2004b) or to increased FPGS activity levels in response to decreased extra- and intracellular folates (Gates et al., 1996), or to direct competitive interactions between polyglutamyl folates and antifolates that substantially interfere with drug binding and inhibition at their enzyme targets, as

Molecular Pharmacology Fast Forward. Published on June 26, 2012 as DOI: 10.1124/mol.112.079004
This article has not been copyedited and formatted. The final version may differ from this version.

documented for MTX (Matherly et al., 1983). Changes in drug efflux are also possible, as ABC transporter (ABCG2, ABCC1) levels and/or intracellular distributions have been described in response to folate deprivation (Ifergan et al., 2005).

In the present study, we found that **C1** and **C2** membrane transport by PCFT was virtually identical between the hRFC-deficient R5 and WT HeLa cell lines. Total and polyglutamyl accumulations of **C1** and **C2** during sustained drug exposures were similar between WT and R5 cells, although there were slight differences in distributions of **C1** and **C2** polyglutamates between the lines. This difference was most pronounced for the longest chain length PGs (PG_5 and PG_6) and appeared to be somewhat greater for **C1** than **C2**. By analogy with other classical antifolates (Mendelsohn et al., 1999; Shih and Thornton, 1999), increased accumulation of long chain polyglutamyl forms of **C1** and **C2** in the R5 subline might result in enhanced inhibition of intracellular GARFTase and *de novo* purine nucleotide biosynthesis (Kugel Desmoulin et al., 2011; Wang et al., 2010; Wang et al., 2011), thus further exacerbating the impact of reduced cellular folate pools in directly competing for GARFTase.

Our results provide proof-of-principle evidence that hRFC levels and function are critical determinants of antitumor activities and *in vivo* efficacies of novel PCFT-targeted antifolates that are not themselves RFC substrates. It is this lack of RFC transport which confers tumor selectivity and decreased toxicity to normal tissues for this novel class of agents. Tumor selectivity would be enhanced by substantial levels of hPCFT protein in solid tumors and by acidic pHs characterizing the tumor microenvironment which favor PCFT over RFC transport (Kugel Desmoulin et al., 2011). Conversely, at neutral pHs

Molecular Pharmacology Fast Forward. Published on June 26, 2012 as DOI: 10.1124/mol.112.079004
This article has not been copyedited and formatted. The final version may differ from this version.

characterizing most normal tissues, RFC transport of reduced folates would be increased, resulting in elevated levels of THF cofactors within cells which further protect from untoward drug effects. Of course, as suggested in this report, in tumors with sufficiently high hRFC, uptake of THF cofactors by this process will likely occur, even at somewhat acidic pHs. Accordingly, any decrease in hRFC function would serve to augment the inherent antitumor selectivities and increase sensitivities to PCFT-selective antifolates.

Molecular Pharmacology Fast Forward. Published on June 26, 2012 as DOI: 10.1124/mol.112.079004
This article has not been copyedited and formatted. The final version may differ from this version.

ACKNOWLEDGEMENTS

We thank Dr. I. David Goldman for his generous gifts of the R5 and R1-11 HeLa cell lines. We thank Ms. Kelly Haagenson for editorial assistance.

AUTHORSHIP CONTRIBUTIONS

Participated in research design: S. Kugel Desmoulin, L. Wang, L. Polin, Z. Hou, A., Gangjee, L.H. Matherly

Conducted experiments: S. Kugel Desmoulin, L. Wang, L. Polin, K. White, J. Kushner, M. Stout, Z. Hou, C. Cherian

Performed data analysis: S. Kugel Desmoulin, L. Wang, L. Polin, M. Stout, Z. Hou, A. Gangjee, L.H. Matherly

Wrote or contributed to the writing of the manuscript: S. Kugel Desmoulin, L. Wang, L. Polin, A. Gangjee, L.H. Matherly

Molecular Pharmacology Fast Forward. Published on June 26, 2012 as DOI: 10.1124/mol.112.079004
This article has not been copyedited and formatted. The final version may differ from this version.

REFERENCES

Alati T, Worzalla JF, Shih C, Bewley JR, Lewis S, Moran RG and Grindey GB (1996) Augmentation of the therapeutic activity of lometrexol -(6-R)5,10-dideazatetrahydrofolate- by oral folic acid. *Cancer Res* **56**(10): 2331-2335.

Anderson CM and Thwaites DT (2010) Hijacking solute carriers for proton-coupled drug transport. *Physiology (Bethesda, Md)* **25**(6): 364-377.

Assaraf YG (2007) Molecular basis of antifolate resistance. *Cancer Metastasis Rev* **26**(1): 153-181.

Assaraf YG and Goldman ID (1997) Loss of folic acid exporter function with markedly augmented folate accumulation in lipophilic antifolate-resistant mammalian cells. *J Biol Chem* **272**(28): 17460-17466.

Chattopadhyay S, Moran RG and Goldman ID (2007) Pemetrexed: biochemical and cellular pharmacology, mechanisms, and clinical applications. *Mol Cancer Ther* **6**(2): 404-417.

Chattopadhyay S, Zhao R, Krupenko SA, Krupenko N and Goldman ID (2006) The inverse relationship between reduced folate carrier function and pemetrexed activity in a human colon cancer cell line. *Mol Cancer Ther* **5**(2): 438-449.

Corbett TH, LoRusso P, Demchick L, Simpson C, Pugh S, White K, Kushner J, Polin L, Meyer J, Czarnecki J, Heilbrun L, Horwitz JP, Gross JL, Behrens CH, Harrison BA, McRipley RJ and Trainor G (1998) Preclinical antitumor efficacy of analogs of XK469: sodium-(2-[4-(7-chloro-2-quinoxalinyloxy)phenoxy]propionate. *Investigational new drugs* **16**(2): 129-139.

Corbett TH, Valeriote FA, Demchik L, Lowichik N, Polin L, Panchapor C, Pugh S, White K, Kushner J, Rake J, Wentland M, Golakoti T, Hetzel C, Ogino J, Patterson G and Moore R (1997) Discovery of cryptophycin-1 and BCN-183577: examples of strategies and problems in the detection of antitumor activity in mice. *Investigational new drugs* **15**(3): 207-218.

Gates SB, Worzalla JF, Shih C, Grindey GB and Mendelsohn LG (1996) Dietary folate and folylpolyglutamate synthetase activity in normal and neoplastic murine tissues and human tumor xenografts. *Biochem Pharmacol* **52**(9): 1477-1479.

Ge Y, Haska CL, LaFiura K, Devidas M, Linda SB, Liu M, Thomas R, Taub JW and Matherly LH (2007) Prognostic role of the reduced folate carrier, the major membrane transporter for methotrexate, in childhood acute lymphoblastic leukemia: a report from the Children's Oncology Group. *Clin Cancer Res* **13**(2 Pt 1): 451-457.

Gibbs DD, Theti DS, Wood N, Green M, Raynaud F, Valenti M, Forster MD, Mitchell F, Bavetsias V, Henderson E and Jackman AL (2005) BGC 945, a novel tumor-selective thymidylate synthase inhibitor targeted to alpha-folate receptor-overexpressing tumors. *Cancer Res* **65**(24): 11721-11728.

Gillies RJ, Raghunand N, Karczmar GS and Bhujwalla ZM (2002) MRI of the tumor microenvironment. *Journal of magnetic resonance imaging : JMRI* **16**(4): 430-450.

Goldman ID, Chattopadhyay S, Zhao R and Moran R (2010) The antifolates: evolution, new agents in the clinic, and how targeting delivery via specific membrane transporters is driving the development of a next generation of folate analogs. *Curr Opin Investig Drugs* **11**(12): 1409-1423.

Goldman ID and Matherly LH (1985) The cellular pharmacology of methotrexate. *Pharmacol Ther* **28**(1): 77-102.

Gorlick R, Goker E, Trippett T, Steinherz P, Elisseyeff Y, Mazumdar M, Flintoff WF and Bertino JR (1997) Defective transport is a common mechanism of acquired methotrexate resistance in acute lymphocytic leukemia and is associated with decreased reduced folate carrier expression. *Blood* **89**(3): 1013-1018.

Guo W, Healey JH, Meyers PA, Ladanyi M, Huvos AG, Bertino JR and Gorlick R (1999) Mechanisms of methotrexate resistance in osteosarcoma. *Clin Cancer Res* **5**(3): 621-627.

Helmlinger G, Yuan F, Dellian M and Jain RK (1997) Interstitial pH and pO2 gradients in solid tumors in vivo: high-resolution measurements reveal a lack of correlation. *Nat Med* **3**(2): 177-182.

Hou Z, Kugel Desmoulin S, Etnyre E, Olive M, Hsiung B, Cherian C, Wloszczynski PA, Moin K and Matherly LH (2011) Identification and functional impact of homo-oligomers of the human proton-coupled folate transporter. *J Biol Chem*.

Ifergan I, Jansen G and Assaraf YG (2005) Cytoplasmic confinement of breast cancer resistance protein (BCRP/ABCG2) as a novel mechanism of adaptation to short-term folate deprivation. *Mol Pharmacol* **67**(4): 1349-1359.

Kugel Desmoulin S, Wang L, Hales E, Polin L, White K, Kushner J, Stout M, Hou Z, Cherian C, Gangjee A and Matherly LH (2011) Therapeutic targeting of a novel 6-substituted pyrrolo [2,3-d]pyrimidine thienoyl antifolate to human solid tumors based on selective uptake by the proton-coupled folate transporter. *Mol Pharmacol* **80**(6): 1096-1107.

Kugel Desmoulin S, Wang Y, Wu J, Stout M, Hou Z, Fulterer A, Chang MH, Romero MF, Cherian C, Gangjee A and Matherly LH (2010) Targeting the proton-coupled folate transporter for selective delivery of 6-substituted pyrrolo[2,3-d]pyrimidine antifolate inhibitors of de novo purine biosynthesis in the chemotherapy of solid tumors. *Mol Pharmacol* **78**(4): 577-587.

Laemmli UK (1970) Cleavage of structural proteins during the assembly of the head of bacteriophage T4. *Nature* **227**(5259): 680-685.

Lowry OH, Rosebrough NJ, Farr AL and Randall RJ (1951) Protein measurement with the Folin phenol reagent. *J Biol Chem* **193**(1): 265-275.

Matherly LH, Barlowe CK, Phillips VM and Goldman ID (1987) The effects on 4-aminoantifolates on 5-formyltetrahydrofolate metabolism in L1210 cells. A biochemical basis of the selectivity of leucovorin rescue. *J Biol Chem* **262**(2): 710-717.

Matherly LH, Czajkowski CA and Angeles SM (1991) Identification of a highly glycosylated methotrexate membrane carrier in K562 human erythroleukemia cells up-regulated for tetrahydrofolate cofactor and methotrexate transport. *Cancer Res* **51**(13): 3420-3426.

Matherly LH, Fry DW and Goldman ID (1983) Role of methotrexate polyglutamylation and cellular energy metabolism in inhibition of methotrexate binding to dihydrofolate reductase by 5-formyltetrahydrofolate in Ehrlich ascites tumor cells in vitro. *Cancer Res* **43**(6): 2694-2699.

Matherly LH, Hou Z and Deng Y (2007) Human reduced folate carrier: translation of basic biology to cancer etiology and therapy. *Cancer Metastasis Rev* **26**(1): 111-128.

Matsudaira P (1987) Sequence from picomole quantities of proteins electroblotted onto polyvinylidene difluoride membranes. *J Biol Chem* **262**(21): 10035-10038.

Mendelsohn LG, Worzalla JF and Walling JM (1999) Preclinical and Clinical Evaluation of the Glycinamide Ribonucleotide Formyltransferase Inhibitors Lometrexol and LY309887, in *Anticancer Drug Development Guide: Antifolate Drugs in Cancer Therapy* (Jackman AL ed) pp 261-280, Humana Press, Inc., Totowa, NJ.

Nimec Z and Galivan J (1983) Regulatory aspects of the glutamylation of methotrexate in cultured hepatoma cells. *Arch Biochem Biophys* **226**(2): 671-680.

Polin L, Corbett TH, Roberts BJ, Lawson AJ, Leopold WR, White K, Kushner J, Hazeldine S, Moore R, Rake J and Horwitz JP (2011) Transplantable Syngeneic Rodent Tumors: Solid Tumors in Mice

Tumor Models in Cancer Research, (Teicher BA ed) pp 43-78, Humana Press.

Polin L, Valeriote F, White K, Panchapor C, Pugh S, Knight J, LoRusso P, Hussain M, Liversidge E, Peltier N, Golakoti T, Patterson G, Moore R and Corbett TH (1997) Treatment of human prostate tumors PC-3 and TSU-PR1 with standard and investigational agents in SCID mice. *Investigational new drugs* **15**(2): 99-108.

Qiu A, Jansen M, Sakaris A, Min SH, Chattopadhyay S, Tsai E, Sandoval C, Zhao R, Akabas MH and Goldman ID (2006) Identification of an intestinal folate transporter and the molecular basis for hereditary folate malabsorption. *Cell* **127**(5): 917-928.

Roberts JD, Poplin EA, Tombes MB, Kyle B, Spicer DV, Grant S, Synold T and Moran R (2000) Weekly lometrexol with daily oral folic acid is appropriate for phase II evaluation. *Cancer Chemother Pharmacol* **45**(2): 103-110.

Shane B (1989) Folylpolyglutamate synthesis and role in the regulation of one-carbon metabolism. *Vitam Horm* **45**: 263-335.

Shih C and Thornton DE (1999) Preclinical Pharmacology Studies and the Clinical Development of a Novel Multitargeted Antifolate, MTA (LY231514), in *Anticancer Drug Development Guide: Antifolate Drugs in Cancer Therapy* (Jackman AL ed) pp 183-201, Humana Press, Inc., Totowa, NJ.

Sirotnak FM, Moccio DM, Kelleher LE and Goutas LJ (1981) Relative frequency and kinetic properties of transport-defective phenotypes among methotrexate-resistant L1210 clonal cell lines derived in vivo. *Cancer Res* **41**(11 Pt 1): 4447-4452.

Tse A, Brigle K, Taylor SM and Moran RG (1998) Mutations in the reduced folate carrier gene which confer dominant resistance to 5,10-dideazatetrahydrofolate. *J Biol Chem* **273**(40): 25953-25960.

Tse A and Moran RG (1998) Cellular folates prevent polyglutamation of 5, 10-dideazatetrahydrofolate. A novel mechanism of resistance to folate antimetabolites. *J Biol Chem* **273**(40): 25944-25952.

Umapathy NS, Gnana-Prakasam JP, Martin PM, Mysona B, Dun Y, Smith SB, Ganapathy V and Prasad PD (2007) Cloning and functional characterization of the proton-coupled electrogenic folate transporter and analysis of its expression in retinal cell types. *Invest Ophthalmol Vis Sci* **48**(11): 5299-5305.

Wang L, Cherian C, Kugel Desmoulin S, Polin L, Deng Y, Wu J, Hou Z, White K, Kushner J, Matherly LH and Gangjee A (2010) Synthesis and antitumor activity of a novel series of 6-substituted pyrrolo[2,3-d]pyrimidine thienoyl antifolate inhibitors of purine biosynthesis with selectivity for high affinity folate receptors and the proton-coupled folate transporter over the reduced folate carrier for cellular entry. *J Med Chem* **53**(3): 1306-1318.

Wang L, Kugel Desmoulin S, Cherian C, Polin L, White K, Kushner J, Fulterer A, Chang MH, Mitchell-Ryan S, Stout M, Romero MF, Hou Z, Matherly LH and Gangjee A (2011) Synthesis, biological, and antitumor activity of a highly potent 6-substituted pyrrolo[2,3-d]pyrimidine thienoyl antifolate inhibitor with proton-coupled folate transporter and folate receptor selectivity over the reduced folate carrier that inhibits beta-glycinamide ribonucleotide formyltransferase. *J Med Chem* **54**(20): 7150-7164.

Webb BA, Chimenti M, Jacobson MP and Barber DL (2011) Dysregulated pH: a perfect storm for cancer progression. *Nature reviews Cancer* **11**(9): 671-677.

Wong SC, McQuade R, Proefke SA, Bhushan A and Matherly LH (1997) Human K562 transfectants expressing high levels of reduced folate carrier but exhibiting low transport activity. *Biochem Pharmacol* **53**(2): 199-206.

Wong SC, Zhang L, Proefke SA, Hukku B and Matherly LH (1998) Gene amplification and increased expression of the reduced folate carrier in transport elevated K562 cells. *Biochem Pharmacol* **55**(7): 1135-1138.

Yang R, Sowers R, Mazza B, Healey JH, Huvos A, Grier H, Bernstein M, Beardsley GP, Krailo MD, Devidas M, Bertino JR, Meyers PA and Gorlick R (2003) Sequence alterations in the reduced folate carrier are observed in osteosarcoma tumor samples. *Clin Cancer Res* **9**(2): 837-844.

Zhao R, Babani S, Gao F, Liu L and Goldman ID (2000a) The mechanism of transport of the multitargeted antifolate (MTA) and its cross-resistance pattern in cells with markedly impaired transport of methotrexate. *Clin Cancer Res* **6**(9): 3687-3695.

Zhao R, Chattopadhyay S, Hanscom M and Goldman ID (2004a) Antifolate resistance in a HeLa cell line associated with impaired transport independent of the reduced folate carrier. *Clin Cancer Res* **10**(24): 8735-8742.

Zhao R, Gao F, Babani S and Goldman ID (2000b) Sensitivity to 5,10-dideazatetrahydrofolate is fully conserved in a murine leukemia cell line highly resistant to methotrexate due to impaired transport mediated by the reduced folate carrier. *Clin Cancer Res* **6**(8): 3304-3311.

Zhao R, Gao F and Goldman ID (2001) Marked suppression of the activity of some, but not all, antifolate compounds by augmentation of folate cofactor pools within tumor cells. *Biochem Pharmacol* **61**(7): 857-865.

Zhao R, Gao F, Hanscom M and Goldman ID (2004b) A prominent low-pH methotrexate transport activity in human solid tumors: contribution to the preservation of methotrexate pharmacologic activity in HeLa cells lacking the reduced folate carrier. *Clin Cancer Res* **10**(2): 718-727.

Zhao R and Goldman ID (2003) Resistance to antifolates. *Oncogene* **22**(47): 7431-7457.

Zhao R and Goldman ID (2007) The molecular identity and characterization of a Proton-coupled Folate Transporter--PCFT; biological ramifications and impact on the activity of pemetrexed. *Cancer Metastasis Rev* **26**(1): 129-139.

Zhao R, Hanscom M, Chattopadhyay S and Goldman ID (2004c) Selective preservation of pemetrexed pharmacological activity in HeLa cells lacking the reduced folate carrier: association with the presence of a secondary transport pathway. *Cancer Res* **64**(9): 3313-3319.

Zhao R, Qiu A, Tsai E, Jansen M, Akabas MH and Goldman ID (2008) The proton-coupled folate transporter: impact on pemetrexed transport and on antifolates activities compared with the reduced folate carrier. *Mol Pharmacol* **74**(3): 854-862.

FOOTNOTES

This study was supported by grants from the National Cancer Institute, National Institutes of Health [CA53535, CA152316, and CA125153], a pilot grant from the Barbara Ann Karmanos Cancer Institute, and a grant from the Mesothelioma Applied Research Foundation. Ms. Kugel Desmoulin was supported by a Doctoral Research Award from the Canadian Institute of Health Research.

L.H. Matherly and A. Gangjee contributed equally to this work.

To whom correspondence should be addressed:
L.H. Matherly, Molecular Therapeutics Program, Barbara Ann Karmanos Cancer Institute, 110 E. Warren Ave, Detroit, MI 48201. Tel.: 313-578-4280; Fax: 313-578-4287; Email: matherly@karmanos.org

A. Gangjee, Division of Medicinal Chemistry, Graduate School of Pharmaceutical Sciences, Duquesne University, 600 Forbes Avenue, Pittsburgh, PA 15282. Tel: 412-396-6070; Fax: 412-396-5593; gangjee@duq.edu

Molecular Pharmacology Fast Forward. Published on June 26, 2012 as DOI: 10.1124/mol.112.079004
This article has not been copyedited and formatted. The final version may differ from this version.

FIGURE LEGENDS

Figure 1. **PCFT expression and function in human solid tumor cell lines.** (*Panel A*) Plasma membrane preparations were isolated as described in Materials and Methods. Membrane proteins (25 μg) from human tumor cell lines were electrophoresed on a 7.5% denaturing polyacrylamide gel and immunoblotted with hPCFT antibody. Na^+/K^+ ATPase protein levels were used as loading controls. hPCFT migrates as a broadly banding species due to its heterogeneous glycosylation. The banding in the lane for the R1-11 HeLa cells is non-specific. The major non-specific band appearing in all lanes is labeled NS. (*Panel B*) Uptake of 0.5 μM [^{3}H]MTX was measured at 37˚C for 5 min in cell monolayers at pH 5.5, as described in Materials and Methods. Internalized [^{3}H]MTX was normalized to total protein. Results are shown for mean values ± standard errors for 3-4 independent experiments. The characteristics of the 14 tumor cell lines are summarized in Table 2S (Supplement).

Figure 2. PCFT transport activity of C2 in R1-11-PCFT4 HeLa cells. (*Panel A*) Structures of 6-substituted pyrrolo[2,3-*d*]pyrimidine thienoyl antifolates **C1** and **C2** (Wang et al., 2010; Wang et al., 2011) are shown. (*Panel B*) Uptake of [^{3}H]**C2** (0. 5 μM) was measured at 37˚C for 5 min at pH 5.5 and 6.8 in the presence or absence of unlabeled **C1** (10 μM). Internalized [^{3}H]**C2** was normalized to total protein. Details are provided in Materials and Methods. Results are shown for mean values ± standard errors for 3 independent experiments.

Figure 3. Characterization of WT and R5 HeLa sublines. (*Panel A*) Representative western blots are shown for sucrose gradient-purified membrane fractions (25 μg) using

Molecular Pharmacology Fast Forward. Published on June 26, 2012 as DOI: 10.1124/mol.112.079004
This article has not been copyedited and formatted. The final version may differ from this version.

hPCFT, hRFC and HA antibodies to detect WT and HA-tagged (R5-RFC^{HA}) proteins. Uptakes of 0.5 μM [^{3}H]MTX, [^{3}H]PMX, [^{3}H]**C1** and [^{3}H]**C2** were measured at 37˚C for 2 min in WT and R5 HeLa cell monolayers at pH 5.5 (*Panel B*) and pH 7.2 *Panel C*). Internalized tritiated drug was normalized to total cellular protein. Experimental details are provided in Materials and Methods. (*Panel D*) The ratios of [^{3}H]MTX uptake at pH 5.5 / pH 7.2 in WT and R5 HeLa cells are plotted. The data in *panels B-D* represent mean values ± standard errors for 3 independent experiments. While there were slight differences in initial rates of uptake for **C1** and **C2** for both WT and R5 HeLa cells in *panel B*, these were not statistically significant ($p>0.1$), consistent with the very modest differences in transport kinetics between these drugs (Table 4S, Supplement)

Figure 4. [^{3}H]5-CHO-THF accumulations in WT and R5 HeLa sublines. Folate-depleted R5 HeLa sublines were treated for 96 h with increasing concentrations of [^{3}H]5-CHO-THF (0-1000 nM) (*Panel A*), or with 25 nM [^{3}H]5-CHO-THF and 0-1000 nM of unlabeled **C1** (*Panel B*) or **C2** (*Panel C*). Internalized [^{3}H]5-CHO-THF was normalized to total cellular proteins. Details are described in Materials and Methods. The data in *panel A* summarize the results as mean values ± standard errors for 3 independent experiments. For each 5-CHO-THF concentration, statistically significant differences were calculated between WT or R5-RFC2 cells, and R5 cells and are noted with * ($p<0.05$) and ** ($p<0.005$). For *panels B and C*, both R5 and WT HeLa cells showed decreased total folate metabolites derived from [^{3}H]5-CHO-THF, accompanying treatment with increased concentrations of **C1** or **C2** (results as mean values ± standard errors for 3-5 independent experiments). The decreases between untreated controls and 1000 nM antifolate treatments were greater for R5 cells than for WT HeLa cells with

Molecular Pharmacology Fast Forward. Published on June 26, 2012 as DOI: 10.1124/mol.112.079004
This article has not been copyedited and formatted. The final version may differ from this version.

both **C1** (decreased 47.1% and 28.1%, respectively; p=0.006) and **C2** (decreased 47.3% versus 29.1%, respectively; p=0.078).

Figure 5. Growth inhibition by antifolate drugs toward WT and R5 HeLa sublines. (*Panel A*) Growth inhibitions were measured by a fluorescence (Cell Titer Blue™)-based assay after 96 h of exposure of folate-depleted WT, R5, R5-mock, and R5-RFC2 HeLa sublines to a range of inhibitor concentrations. Results are presented as 50% inhibitory concentrations (IC_{50}s) as mean IC_{50} values ± standard errors from 5-12 independent experiments. IC_{50} values are summarized in Table 5S (Supplement). Statistically significant differences between results for WT HeLa or R5-RFC2 cells and those for R5 cells are noted with a * ($p<0.01$). For **C1** (*Panel B*) and **C2** (*Panel C*), growth inhibition experiments were performed in the presence of increasing concentrations (25, 100, 1000 nM) of extracellular 5-CHO-THF. Results are summarized as mean IC_{50} values ± standard errors from 3-11 independent experiments. Statistically significant differences between results for WT HeLa and those for R5 HeLa cells are noted with a * ($p<0.005$).

Table 1. Antitumor Efficacy Evaluation of C1 and C2 Against Early Stage Human R5 and HeLa in Female SCID Mice.

Tumor	Agent	Total dose (mg/kg)	Median tumor mass in mg (range) on day 21	T/C (%)	Time to 1000mg in days (range)	T-C (days)	Gross Log_{10} kill	Activity rating
R5	No Treatment	–	1054 (916 – 1272)	–	21 (20-22)	–	–	–
	C1	720	0 (all zeroes)	0	44 (39-49)	23	3.3	++++
	C2	128	32 (0 – 75)	3	38.5 (36-42)	17.5	2.5	+++
HeLa	No Treatment	–	1009 (847 – 1701)	–	21 (18-22)	–	–	–
	C1	720	63 (0 – 247)	6	34 (31-37)	13	1.9	++
	C2	128	69 (0 – 189)	7	34 (30-40)	13	1.9	++

The 8-week old female NCR SCID mice were implanted bilaterally subcutaneously with 30-60 mg tumor fragments by a 12-gauge trocar on day 0. Both tumor studies (WT and R5 HeLa cells) used 4 mice per group. Median mouse body weights for each experiment were within 2 g and were 19 g (WT) or 19.5 g (R5) HeLa at the start of therapy. Chemotherapy was started on day 3 after tumor implantation, when the numbers of cells were small ($10^7 – 10^8$ cells). To determine the T/C value, the treatment and control groups were measured when the control group tumors reached approximately 700-1200 mg in size (median of group). The median tumor weight of each group was determined (including zeros). The T/C value is an indication of antitumor effectiveness. A T/C equal to or less than 42% is considered significant antitumor activity by the Drug Evaluation Barancgh of the Division of Cancer Treatment (NCI). A T/C value <10% is considered to indicate highly significant antitumor activity, and is the level used by NCI to justify a clinical trial if toxicity, formulation, and certain other requirements are met. Day 0 = day of tumor implant A T/C = 0 indicates very high antitumor activity. The relationship between log_{10} tumor cell kill and the activity rating is as follows: > 2.8 log_{10} kill (highly active ++++); 2.0 - 2.8 (+++); 1.3 – 1.9 (++); 0.7 – 1.2 (+); < 0.7 (Inactive –). Statistical analyses were performed for the differences in T-C and log_{10} kills between WT HeLa and R5 HeLa cells for **C1** and **C2** relative to the median control values for each tumor. Differences in T-C and log_{10} kill results between R5 and WT HeLa cells for compound **C1** were statistically significant (p=0.014 and p=0.0135, respectively). While these parameters also differed for **C2** between the cell lines, these differences did not quite reach statistical significance (p=0.146).

Molecular Pharmacology Fast Forward. Published on June 26, 2012 as DOI: 10.1124/mol.112.079004
This article has not been copyedited and formatted. The final version may differ from this version.

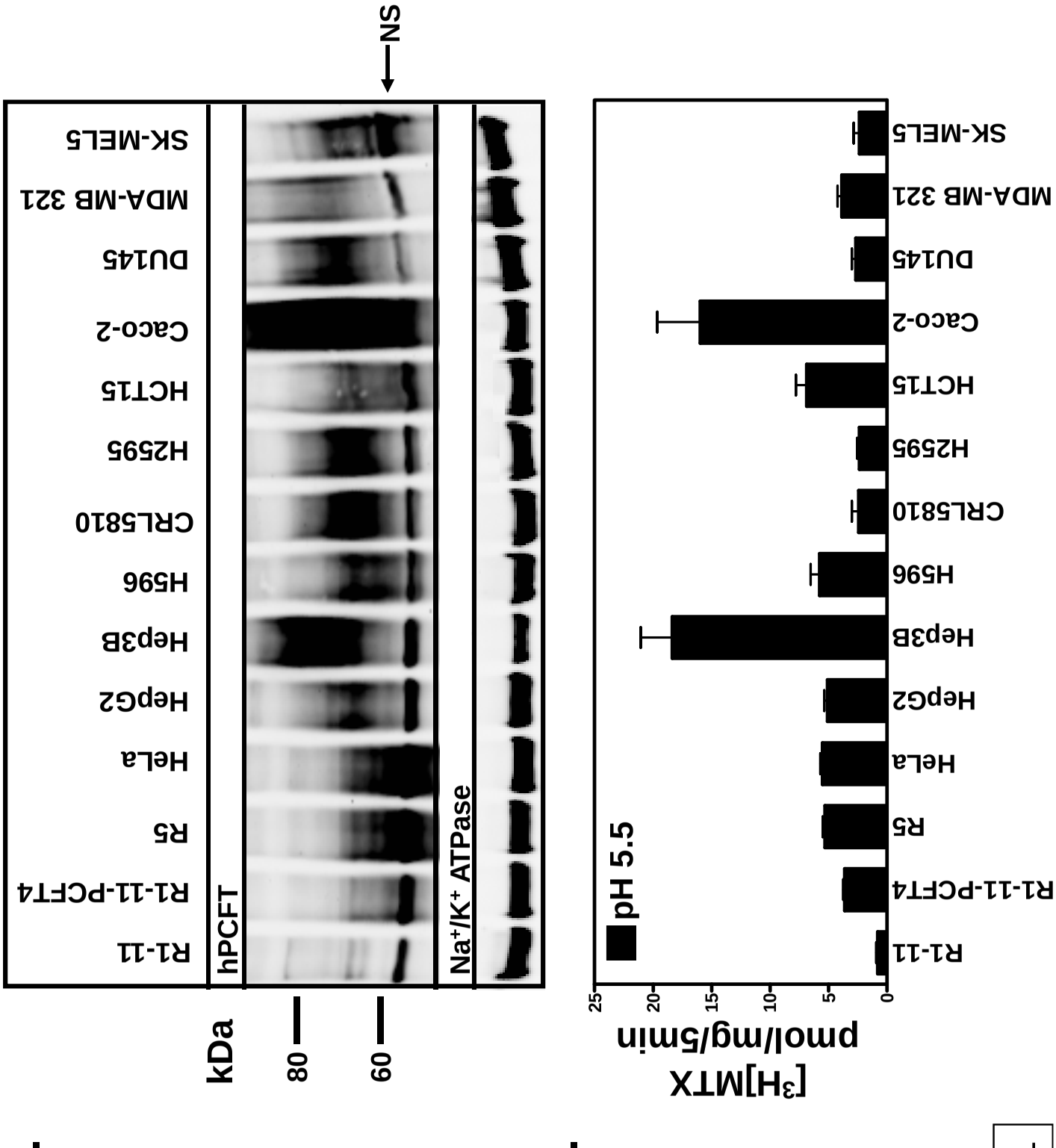

Figure 1

A.

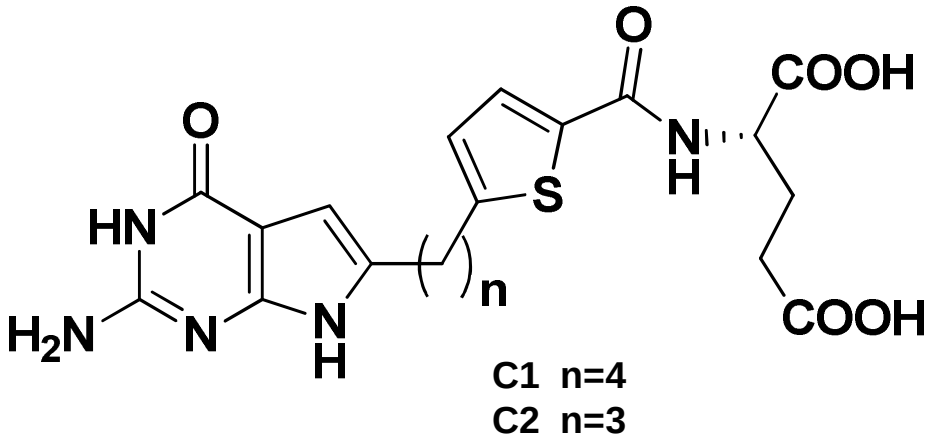

B.

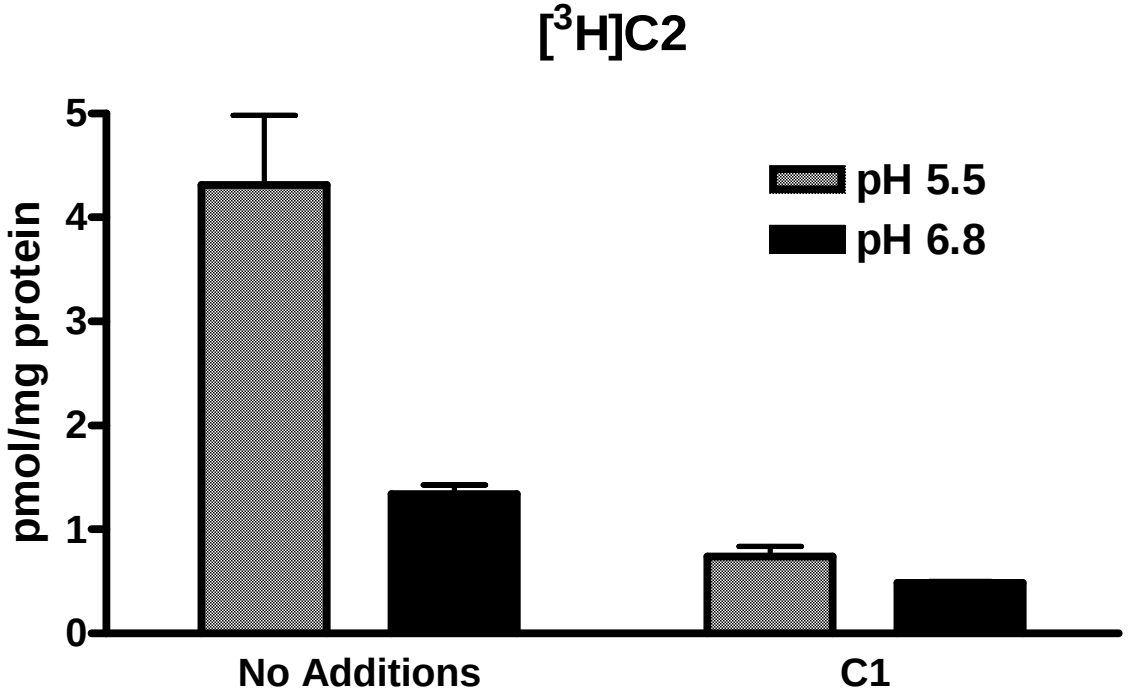

Figure 2

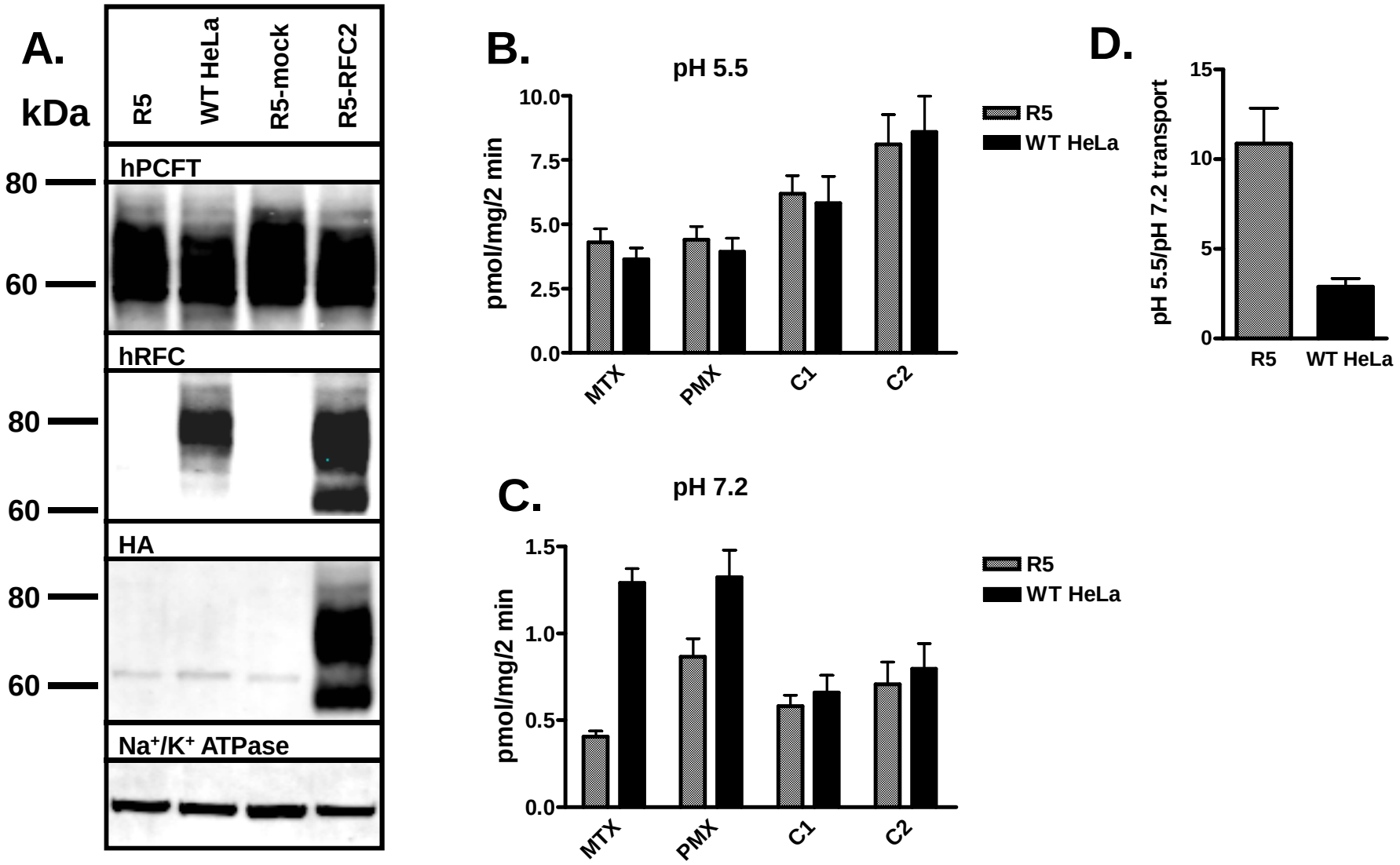

Figure 3

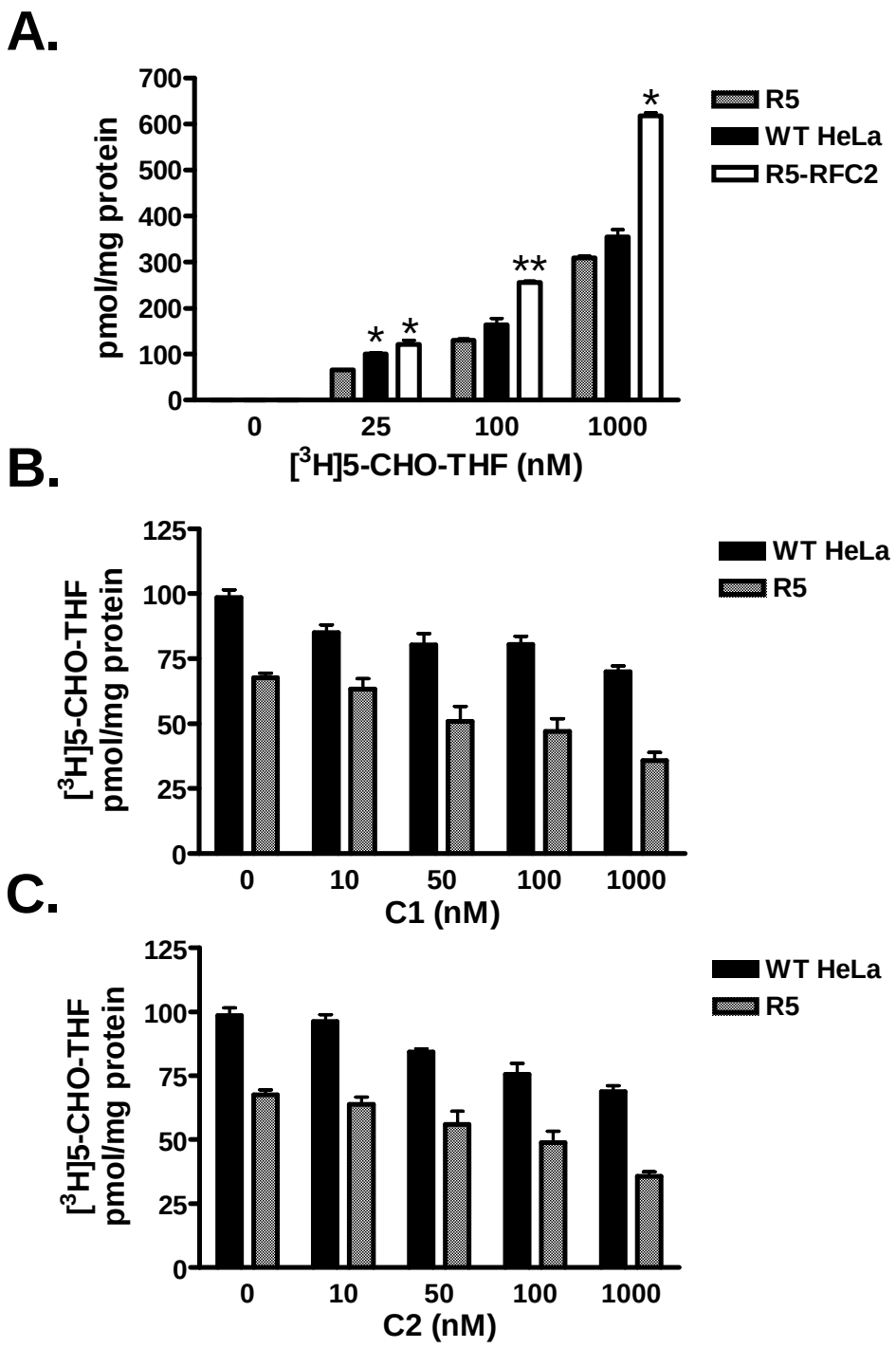

Figure 4

Figure 5